

The role of current layers in magnetic field stochasticization

H.J. de Blank and V. Zhukov*

*FOM-Instituut voor Plasmafysica, Association Euratom-FOM,
Trilateral Euregio Cluster, P.O. Box 1207, 3430 BE Nieuwegein, The Netherlands*

** Institute of Computational Technologies, Lavrentjeva Ave., 6 Novosibirsk, 630090, Russia*

Introduction. The design of the dynamic ergodic divertor (DED) for the TEXTOR tokamak entails time-dependent currents in a helical coil system to produce magnetic perturbations that are resonant at the $q=3$ surface inside the plasma [1]. The perturbations can break up the $q=3$ and nearby equilibrium flux surfaces to create a stochastic field. In the absence of perturbed plasma currents, at times much longer than the resistive time, the stochastic magnetic field is the superposition of the equilibrium field and the vacuum field produced by the ergodic divertor coils.

The present paper concerns shorter timescales, on which the localized plasma currents induced by the perturbation field play a role. The penetration of the perturbation field strongly depends on the radial distribution of these currents [2]. The toroidal phase velocity of the DED perturbations are found to have a strong effect on their penetration into the plasma. Moreover, through the plasma resistivity the DED fields also apply a torque to the plasma, and the resulting plasma spin-up also affects the field penetration. These compound effects have been studied numerically using a 2-dimensional (poloidal) slab model, and an overview is given here.

The model. On a 2-dimensional domain $0 < x < 1$, $0 < y < y_0$ ($y_0 = 10$) perpendicular to a dominant magnetic field component we consider the reduced MHD equations,

$$\begin{aligned}\partial_t \psi + \mathbf{v} \cdot \nabla \psi &= \eta(\Delta \psi - 1), \\ \partial_t \mathbf{v} + \mathbf{v} \cdot \nabla \mathbf{v} &= \nu \Delta \mathbf{v} - \Delta \psi \nabla \psi - \nabla p, \\ \nabla \cdot \mathbf{v} &= 0.\end{aligned}\tag{1}$$

Note that this model does not include fast magnetosonic waves, which have been also considered as the mechanism for DED field penetration [3]. Initial conditions are $\mathbf{v} = 0$, $\psi_0 = \frac{1}{2}x^2$ (with neutral surface at $x = 0$). Boundary conditions are: periodicity $y \rightarrow y + y_0$, symmetry of ψ in the neutral line $x = 0$, and at $x = 1$ the plasma edge is modeled by $v_x = 0$, $\partial_x v_y = 0$. Quantities are normalized to the box size $x = 1$, the poloidal Alfvén speed, and the poloidal field $\partial_x \psi_0(x = 1) = 1$. We consider a constant viscosity ν and a resistivity which is almost constant, η_p , throughout most of the domain but increases to a large value $\eta_e \gg \eta_p$ at the edge according to $\eta(x) = \eta_p + \eta_e \exp(-(x-1)^2/b^2)$, with $b = 0.07$, $\eta_p = 2 \cdot 10^{-3}$ and $\eta_e = 0.1$. At the edge a magnetic perturbation is propagating in the y -direction with a velocity v_p ,

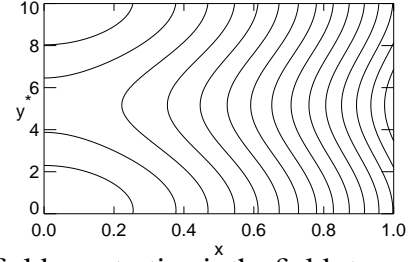
$$\psi(x = 1) = \frac{1}{2} - \psi_p(1 - e^{-t/t_0}) \cos(2\pi y^*/y_0),\tag{2}$$

where $y^* \equiv y - v_p t$ and where $t_0 = 10$ is the initial rise time of the perturbation.

Stationary state For $t \rightarrow \infty$ the system approaches the co-rotating stationary state with $v_x = 0$, $v_y = v_p$, and $\psi = \psi_\infty$ (see Fig. 1) which is the MHD-stable solution of the equation $\Delta \psi_\infty = 1$ (no perturbed current) with boundary condition $\psi_\infty(x = 1) = \frac{1}{2} - \psi_p \cos(2\pi y^*/y_0)$:

Fig. 1: The steady-state flux function ψ_∞ for $\psi_p = 0.05$, given by

$$\psi_\infty = \frac{1}{2}x^2 - \psi_p \cos\left(\frac{2\pi y^*}{y_0}\right) \frac{\cosh(2\pi x/y_0)}{\cosh(2\pi/y_0)}$$



For a system approaching this steady state, a measure for the field penetration is the field strength on the neutral line normalized to the value at $t = \infty$, $\hat{B}_x = (2\pi\psi_p)^{-1}y_0 \cosh(2\pi/y_0) \max_{x=0} \partial_y \psi$. The evolution of the plasma velocity towards the co-rotating steady state $v_y = v_p$ is monitored by three normalized quantities, the maximum velocity on the domain $\hat{v}_m = \max v_y/v_p$, the average over the domain $\langle \hat{v}_y \rangle = y_0^{-1} \int \int dx dy v_y/v_p$, and the average over the neutral line $\langle \hat{v}_c \rangle = y_0^{-1} \int dy v_y(x=0)/v_p$. The current perturbation is characterized by J_m and J_c , defined as the maximal values of $|J_z - 1|$ on the entire domain and on the axis $x = 0$, respectively.

The magnetic field penetration proceeds in entirely different ways in the sub-Alfvénic case $v_p < 1$ and the trans-Alfvénic case $v_p > 1$, which are treated separately.

Field penetration for $v_p < 1$. A sub-Alfvénic running perturbation causes the immediate formation of a current sheet on the resonant surface $x = 0$ (Fig. 2), just as in the case $v_p = 0$. The penetration process strongly depends on the amplitude ψ_p because the plasma acceleration depends nonlinearly on the amplitude, $\partial_t \langle v_y \rangle = -\langle \Delta \psi \partial_y \psi \rangle + \dots \sim \psi_p^2$. From a simplified description of a stationary skin current, $(v_p - v_y) \partial_y \psi = \eta \Delta \psi$, one finds the scaling $\langle \Delta \psi \partial_y \psi \rangle \sim \psi_p^2 \eta^{1/2} (v_p - v_y)^{-1/2}$. The full model (2) is more complex, e.g. because the averaged force on the plasma $\langle \Delta \psi \partial_y \psi \rangle$ also depends on the phase-difference in y between $\Delta \psi$ and $\partial_y \psi$. However, the conclusion remains true that larger ψ_p , larger η_p , and smaller v_p all lead to a faster perturbed field penetration.

Initially, the plasma is accelerated mostly in the resonant layer. The acceleration of the plasma away from $x = 0$ is slower. The decay of the resonant current sheet speeds up when $v_p - v_y$ decreases and becomes comparable to η_p , as can be seen from the increase of \hat{B}_x in Fig. 2a. A larger viscosity results in a somewhat slower penetration because viscosity tends to slow down the resonant plasma layer.

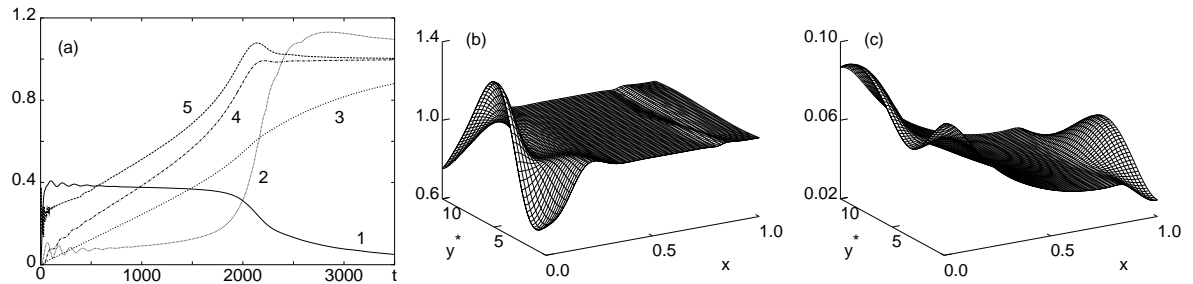


Fig. 2: Sub-Alfvénic case $v_p=0.1$, $\psi_p=0.025$. $\nu=2 \cdot 10^{-4}$; evolution of J_c (a1), \hat{B}_x (a2), $\langle \hat{v}_y \rangle$ (a3), $\langle \hat{v}_c \rangle$ (a4), and \hat{v}_m (a5); distribution of the current J_z (b) and velocity v_y (c) at intermediate stage $t=1900$.

Field penetration for $v_p > 1$. While for $v_p < 1$ the plasma accelerates first at $x = 0$ and later near the edge, in the trans-Alfvénic case $v_p > 1$ it is the other way around: firstly, a skin current sheet is formed near the edge $x = 1$ (phase I) accompanied by an acceleration of the

plasma near the edge. Subsequently, this plasma motion penetrates deeper into the plasma due to viscosity.

The further evolution (phase II) depends on the profile of v_y . If this profile remains sufficiently smooth, the subsequent behaviour is as illustrated in Fig. (3), a case with large viscosity, $\nu = 10^{-3}$. When $v_p - v_y$ drops below the Alfvén velocity at the resonant layer $x = 0$, the current starts to penetrate into the plasma (at $t = 1900$, see Fig. 3). As a consequence, the plasma acceleration increases in the entire domain.

As soon as $v_p - v_y < 1$ everywhere ($t = 2500$) the situation is analogous to the case $v_p < 1$: the current sheet at $x = 0$ is formed, only to decay again as soon as $v_p - v_y \sim \eta_p$. Then \hat{B}_x begins to increase and the configuration tends to its final state.

At smaller ψ_p , both phase I and II take longer. Larger v_p prolongs phase I because of the slower acceleration but has little effect on phase II because this phase always begins when $v_p - v_y \approx 1$, irrespective of the value of v_p . Contrary to the sub-Alfvénic case, for $v_p > 1$ a larger viscosity speeds up the penetration process because it enhances the penetration of v_y from the edge in phase I. This effect more than compensates for the extra drag on the plasma in the current sheets at $x = 1$ (phase I) and $x = 0$ (phase II) by viscosity. The resistivity η_p has only a weak effect in phase I (when the current is concentrated in the edge region where $\eta \gg \eta_p$), but in phase II a smaller η_p slows down the decay of the current sheet at $x = 0$.

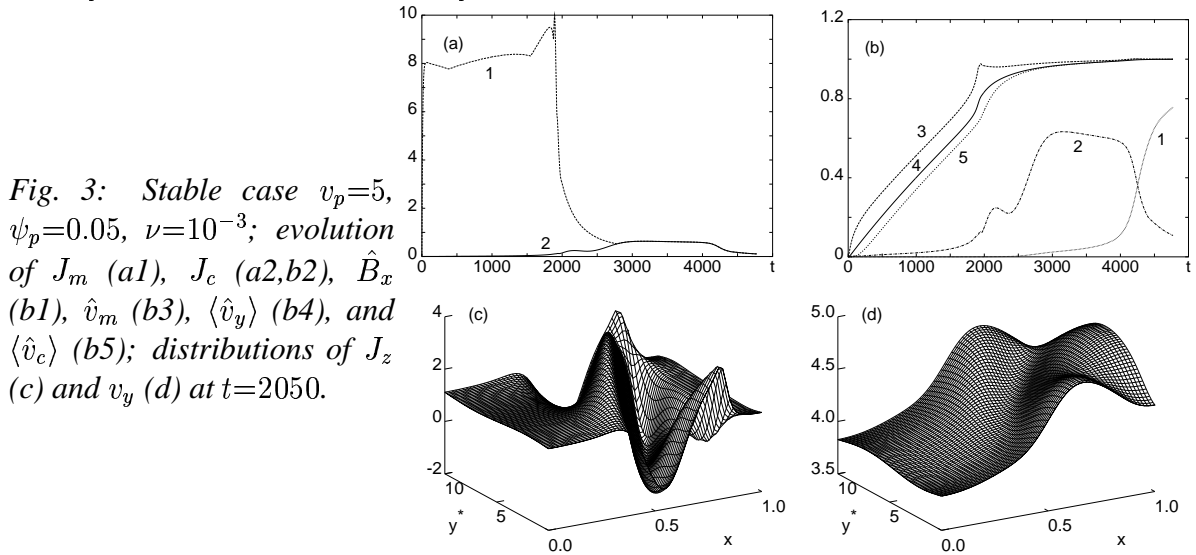


Fig. 3: Stable case $v_p=5$, $\psi_p=0.05$, $\nu=10^{-3}$; evolution of J_m (a1), J_c (a2,b2), \hat{B}_x (b1), \hat{v}_m (b3), $\langle \hat{v}_y \rangle$ (b4), and $\langle \hat{v}_c \rangle$ (b5); distributions of J_z (c) and v_y (d) at $t=2050$.

Instability for $v_p > 1$. If the gradient of v_y at the end of phase I is large, a high frequency small wavelength instability occurs. For $v_p > 1$, this velocity shear instability is not stabilized by the magnetic field. Note that our numerical model is 2-dimensional. Adding a third (e.g. ignorable) coordinate may give rise to further instabilities.

The consequences of the instability depend on when the instability occurs. For small viscosity (e.g. $\nu = 5 \cdot 10^{-4}$, see Fig. 4), ∇v_y grows fast and a strong instability takes place before $v_p - v_y < 1$. It perturbs the entire domain (Fig. 4d,e,f) and causes a fast penetration of J_z everywhere. As the instability decays, a fast convergence of v_y to v_p everywhere leads to the final stationary state without going through the phase with a current sheet at $x = 0$.

For slightly higher viscosity ($\nu = 7.5 \cdot 10^{-4}$), the instability takes place after $v_p - v_y < 1$ and is much weaker. Though the instability causes magnetic perturbations in the plasma comparable to the edge perturbation ψ_p , the instability has a shorter wavelength and does not lead to the fast current penetration seen for smaller viscosity. Hence the further evolution, with current

sheet formation at $x = 0$, is similar to the case without instability in Fig. 3.

The onset of instability is largely determined by the value of ∇v_y , which obviously depends on ν . For smaller ψ_p , phase I takes longer, giving viscosity more time to reduce ∇v_y . Also a larger value of v_p slows down the plasma acceleration and thus reduces ∇v_y . However, eventually v_y grows to a larger value, and ∇v_y as well. Hence the larger v_p delays the instability but does not prevent it.

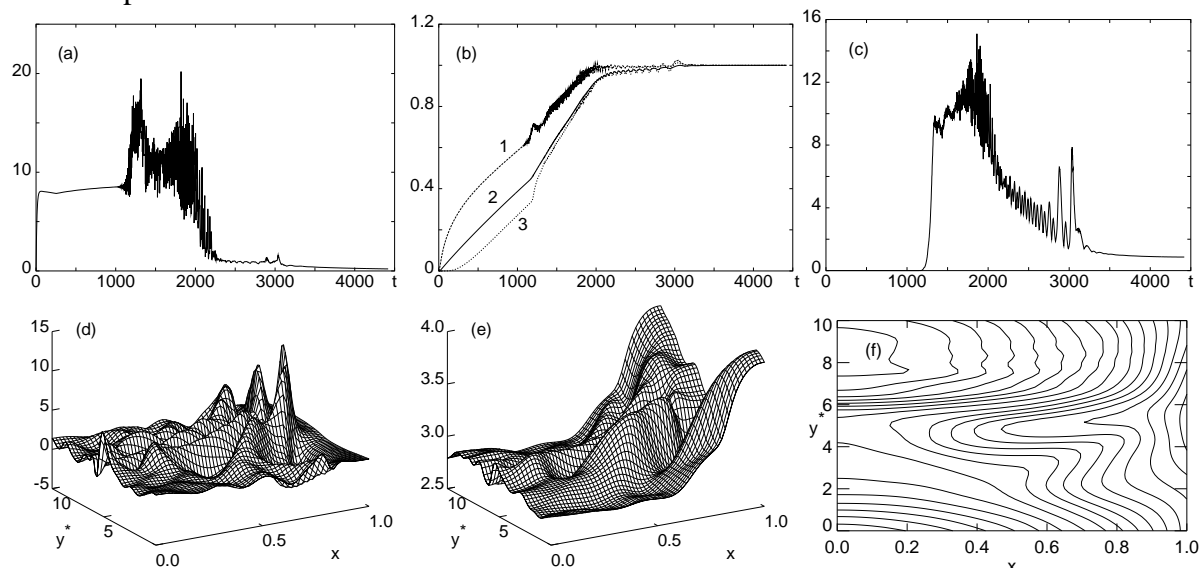


Fig. 4: Strongly unstable case with $v_p=5$, $\psi_p=0.05$, $\nu=5 \cdot 10^{-4}$; evolution of J_m (a), \hat{v}_m (b1), $\langle \hat{v}_y \rangle$ (b2), $\langle \hat{v}_y \rangle$ (b3), and \hat{B}_x (c); the distributions of J_z (d), v_y (e) and ψ (f) at $t=1400$.

Conclusions.

1. The penetration of a running magnetic field perturbation into the plasma depends strongly and nonlinearly on its amplitude.
2. The plasma acceleration plays an important role in this penetration process: complete field penetration is reached only after the plasma velocity has approached the perturbation phase velocity.
3. For $v_p < 1$ and for $v_p > 1$ very different penetration processes are found. In the latter case a velocity-shear instability can arise.
4. The dependence of the penetration process on plasma parameters could help the determination of transport coefficients and measurements of the plasma velocity.
5. Penetration of a rotating field is a promising method for plasma spin-up: a very smooth velocity profile can be produced, controlled accurately by v_p . The required magnetic field perturbation can be quite small.

Acknowledgments. This work was performed under the Euratom-FOM Association agreement with financial support from NWO and Euratom.

References.

- [1] A. Kaleck, M. Hassler, and T. Evans, Fusion Eng. Des. **37**, 353 (1997).
- [2] K.H. Finken, Nucl. Fusion **39**, 707 (1999).
- [3] D.W. Falkoner and R. Koch, Fusion Eng. Des. **37**, 399 (1997).